Nuclear Instruments and Methods in Physics Research A 841 (2017) 34–46

Contents lists available at ScienceDirect

Nuclear Instruments and Methods in Physics Research A

journal homepage: www.elsevier.com/locate/nima

HERITAGE: the concept of a giant flux neutron reflectometer for the exploration of 3-d structure of free-liquid and solid interfaces in thin films

S. Mattauch[a,*], A. Ioffe[a], D. Lott[b], L. Bottyán[c], J. Daillant[d], M. Markó[c], A. Menelle[e], S. Sajti[c], T. Veres[c]

[a] JCNS at MLZ, Forschungszentrum-Jülich GmbH, 85747 Garching, Germany
[b] Helmholtz Zentrum Geesthacht, 21502 Geesthacht, Germany
[c] Wigner Research Center for Physics, 1525 Budapest, Hungary
[d] Synchrotron Soleil L'Orme des Merisiers Saint-Aubin, BP 48 91192 Gif-sur-Yvette, France
[e] Laboratoire Léon Brillouin CEA/CNRS, CEA Saclay, 91191 Gif sur Yvette, France

ARTICLE INFO

Keywords:
Neutron instrumentation
Reflectometry
Focusing GISANS
Polarised neutrons
Free standing liquid interfaces
Kinetics

ABSTRACT

The instrumental concept of HERITAGE – a reflectometer with a horizontal sample geometry – well fitted to the long pulse structure of a neutron source is presented. It is constitutes a new class of reflectometers achieving the unprecedentedly high flux for classical specular reflectometry combined with off-specular reflectometry and grazing incidence small-angle scattering (GISANS), thus resulting in a complete 3-d exploration of lateral and in depth structures in thin films. This is achieved by specially designed neutron guides. In the horizontal direction (perpendicular to the scattering plane) the guide's elliptic shape focusses the neutrons onto the sample. In the vertical direction a multichannel geometry provides a smooth divergence distribution at the sample position while accepting the entire beam from a compact high-brilliance flat moderator.

The modular collimation setup of HERITAGE provides extremely high flexibility in respect to sample geometries and environments, including the possibility to study virtually all types of solid and liquid interfaces, statically or kinetically. The use of multiple beam illumination allows for reflectivity and GISANS measurements at liquid interfaces both from above and below without a need to move the sample.

This concept assures the delivery of the maximum possible and usable flux to the sample in both reflectivity and GISANS measurement regimes. The presented design outperforms the flux of all present-day and already for the ESS planned reflectometers and GISANS setups in flux and in measuring time for standard samples.

1. Introduction

The decision on the construction of the European Spallation Source (ESS) initiated a number of studies on the instrumentation for a long pulse neutron source. It will provide an exciting opportunity to design a reflectometer of the next generation to meet the increasing demand and anticipated scientific challenges [1]. In several meetings and in two specialized workshops carried out in 2012 and 2013, internationally recognized experts in the field of soft and hard matter discussed the science case for neutron reflectometry at the ESS. They identified the scientific drivers in which neutron reflectometry will assist in gaining valuable and unique information when the ESS starts its operation. The anticipated research topics comprise a wide range of scientific disciplines, ranging from thin film magnetism and novel topological phases in confined geometries, over the functionality and properties of hybrid materials in both soft and hard matter science to the structural biology of membrane proteins. A particular focus was put on the increasing complexity of thin film samples involving depth resolved two-dimensional patterning (exploration of 3-d structures in thin films) to enhance performance and create new functionalities as well as on the realisation that nanoscale lateral structures of "natural" interfaces in soft matter are essential for their functionality.

Despite the growing number and steady advancements of neutron reflectometers in the last decades all around the world neutron reflectometry research still experiences serious restrictions that handicap the use of this technique for addressing the discussed science case in its full extent. The biggest drawback here is the generally low neutron flux available even at the nowadays strongest neutron sources which limits the accessible Q-range and thus the spatial resolution of the information gained from specular as well as from off-specular neutron reflectivity. Another restriction consists in the limited flexibility of the existing instruments allowing in general only one

* Corresponding author.
E-mail address: s.mattauch@fz-juelich.de (S. Mattauch).

http://dx.doi.org/10.1016/j.nima.2016.09.043
Received 10 May 2016; Received in revised form 16 September 2016; Accepted 19 September 2016
Available online 29 September 2016

application of a particular operation mode in one experimental setup of the instrument. If, for example, the 3-d structure of a thin film sample is investigated, it is desired to provide a fast and easy switch between specular, off-specular and GISANS mode. Moreover, for free liquid samples it is important to allow for measurements in a wide Q-range, i.e. by applying different angles of incidence, without being forced to move the sample, since any additional movement may influence the properties of the sample or require long waiting times for the relaxation to the original state. The requirements on a neutron reflectometer free from the above limitations can be summarized as follows: it should provide the highest possible intensity for GISANS and standard reflectivity mode and be built in the horizontal sample geometry to account for – beside other systems – the increasing demand for studies of free standing liquid interfaces. Furthermore it should foster the compatibility of the different types of measurements carried out on one sample at set external parameters. It should have a flexible wavelength resolution from 1% to 10% for tuning the Q-resolution in respect to the scientific needs. It should enable to relax it to gain on flux for Q-resolutions in the regime of small length scales, but for specular reflectivity of thicker layers and for GISANS of larger lateral structures (several hundred nanometres) or for allowing precise depth sensitivity in the TOF-GISANS mode, it should leave the Q-resolution adjustable. Its wavelength band should be chosen as wide as possible for the investigation of fast reactions and processes to probe e.g. kinetics of self-assembly of colloidal particles, folding of proteins or in-situ investigation of the exchange processes in membranes. It should have full polarisation capability, i.e. a polarised beam with subsequent polarisation analysis, is required for the measurements of magnetic samples. Moreover, this polarisation capability may also be available for the soft matter samples to reduce incoherent background or to enhance the contrast by using a magnetic reference layer. The beam size needs to be optimized for typical sample sizes of 10×10 mm^2 and 5×5 mm^2 the typical size of high quality samples produced by molecular beam epitaxy or pulsed laser deposition. Since in soft matter, but also certain hard matter samples will anyway be available with larger surface areas, the instruments should also allow one to make use of the larger amount of scattering material. Thanks to a new flat (also called “pancake”) cold moderator [2] planned to be installed at the ESS, the neutron beams will have 2.5–3 times higher brilliance in comparison with standard cold TDR moderators. As a result the peak intensity of the ESS is expected to be about 60–75 times higher than the intensity of the time-of-flight instruments at the ILL. This opens an exciting opportunity to design a reflectometer of the next generation to meet the increasing demand and anticipated scientific challenges.

HERITAGE is an instrument concept dedicated to studies of 3-dimensional structures in thin films fulfilling the list of the above requirements with best performance. Being designed for studies of both free-liquid and solid interfaces, HERITAGE possesses also all operation modes conceivable for a liquid reflectometer, including fast kinetic studies of liquid samples without the necessity of sample motion in neither case of illumination-from-above or -below.

As we will show below, the unprecedentedly high flux of HERITAGE due to its optimized focussing elliptic neutron guide in the horizontal plane allows for studies of very thin films and interfacial regimes, down to 5 Å. The high flux can be traded for very high Q_z-resolution required for example in depth-profiling that is currently only possible by X-rays and is a blind spot for neutrons due to the limited intensity of present neutron instruments.

The broad overlap of the accessible lateral length scales of multi-beam focussing GISANS and off-specular reflectometry permit studies of lateral structures in an extremely wide range from 0.4 to 30 μm. All the above allow for a gap-less exploration of the Q-space of thin interfaces in all 3 directions.

The full polarisation analysis in combination with the high flux will push the limits of signal to noise ratio for samples with inherent incoherent scattering since those studies were not possible before due to background issues.

With these characteristics the HERITAGE design meets most requirements formulated in the science case of ESS reflectometry. Apart from very small (below 1 mm^2) samples the present HERITAGE design satisfies all foreseeable ambitions of the biological, hard matter and soft matter community.

2. General philosophy: relaxed *Q*-resolution machine

Investigations of thin interfaces (from several nm down to the sub nm range) require a delivery of as much usable intensity as possible to the sample position being able to access a dynamic range of 8 orders of magnitude or more (see Section 11). As the instrument is dedicated to the investigation of thin interfaces from 5 Å (Q=2π/5 Å=1.25 Å^{-1}) on the wavelength resolution can be relaxed to $\Delta\lambda/\lambda=10\%$ to without any loss of information. Indeed, with a relaxed resolution the neutron intensity on the sample is significantly increased to obtain a detectable signal even from an extremely small amount of scattering material of a thin layer, in particular, , when reflectivity is required to measure up to high Q values. The pulse width τ and the instrument length L from the moderator to detector impose physical limits on the main instrument parameters – the natural Q-resolution and the wavelength band $\Delta\lambda$, both are directly determined by the choice of τ and L:

$$\frac{\Delta Q}{Q} \propto \frac{\tau}{T} \propto \frac{\tau}{L} \quad \Delta\lambda \propto \frac{1}{L} \tag{1}$$

where T is the flight time of the neutrons from the moderator to the detector. To achieve a wavelength resolution of 10% for τ=2.86 ms at the ESS and to use the maximum number of neutrons from the spectrum centred around the wavelength of 3 Å, the instrument length L is fixed at about 36 m. When L is fixed no further relaxation of the wavelength resolution is possible. However an increase in the resolution can be achieved by artificially shortening the pulse length. In turn the repetition rate of 14 Hz and the choice of instrument length defines the wavelength band of the instrument to $\Delta\lambda$=8 Å.

3. General instrument layout

Recent moderator developments at the ESS resulted in the discovery of low-dimensional para-H_2 pancake moderators [3] allowing for a brilliance (i.e. phase density) gain of up to an order of magnitude in comparison with a standard moderator. Such pancake moderators should certainly provide a significant intensity gain for neutron instruments with high Q-resolution, as e.g. for small-angle scattering diffractometers and reflectometers which require highly collimated beams (i.e. the selection of a small volume of the phase space).

Neutron reflectometry relies on a beam of smooth and flat divergence profile in the scattering plane. The low dimensional ESS moderator provides neutrons for a number of neutron beams, consequently its optimum form is of a flat disc (pancake) with a height of about 3 cm [2,3]. Using a neutron guide with the same height (3 cm in the case of HERITAGE), however, results in an incomplete filling of the phase space of neutrons accepted by the neutron guide. Moreover it has a rather irregular divergence profile (see Fig. 1) at the exit of the neutron guide (in front of the collimation). Such an irregular divergence profile is hardly usable for neutron reflectometry.

This obstacle is in general overcome by reducing the height of neutron guide by keeping it 3–5 times smaller than the height of the moderator. We achieve this by splitting the 3 cm height neutron guide into 5 equidistant horizontal channels with heights of 6 mm each (Fig. 2, see also Table 1). Such a design results in a smooth divergence profile (see Fig. 8 in Section 5) necessary for the use of the multibeam illumination system (Section 4). It further allows for taking advantage of the enhanced brilliance of the flat moderator, while keeping a large total cross-section of the neutron guide in the flat direction and thus accepting a high neutron flux from the source.

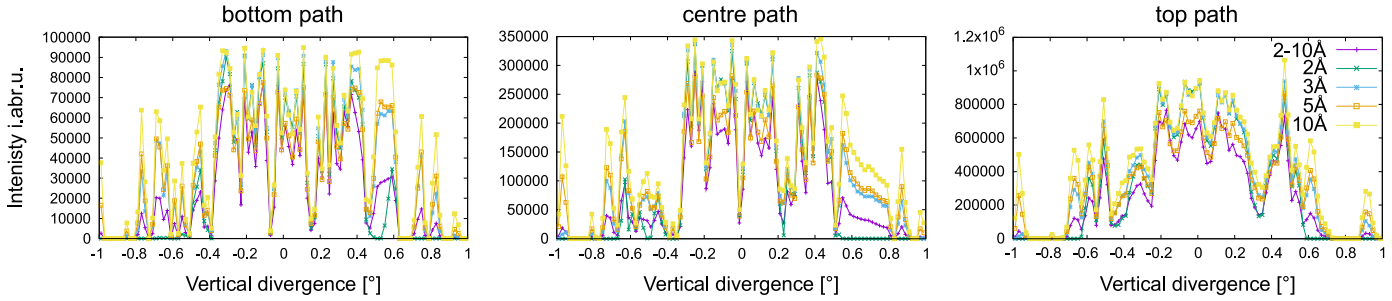

Fig. 1. Divergence profiles of 3 beams at the entrance of the "Liquid-Nose" (discussed in Section 5.1) for a non-channelled guide illuminated by a 3 cm pancake moderator. The plots for the different wavelengths are scaled to each other.

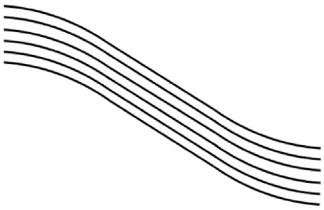

Fig. 2. Five channel S-guide in basic configuration.

The layout of HERITAGE is presented in Fig. 3. In the vertical plane the instrument guide is of S-shape made of two 10 m long curved neutron guides (R=400 m) with a 7 m long straight section around the inflection point (see Fig. 2). The 2nd line of sight is lost at 24 m distance from the moderator that is 10 m upstream the sample position, so that the direct view of primary and secondary radiation sources is well avoided. The neutron guide is inclined by 2° with respect to the floor to allow for studying free liquid surfaces. The channel structure of the neutron guide will have a gap in the centre of the straight section 16 m downstream the neutron beam, where the movable transmission polariser is placed (details in Section 7).

In the vertical (scattering) plane the neutron guide ends 4.5 m upstream of the sample to provide a 4 m long slot for the collimation options of the beam. In the horizontal plane, the elliptic neutron guide extends up to 0.5 m upstream of the sample. The last 4 m of this section (shown by the brown dash lines in the top view of Fig. 3) can be modularly exchanged to provide different collimation options for the operational modes of HERITAGE described in Section 8. Basic guide parameters are listed in Table 1.

In the horizontal plane, the neutron guide is of elliptic shape with the focal points on the moderator and the sample. It allows focussing a divergent neutron beam onto the sample in the horizontal plane (i.e. perpendicular to the vertical scattering plane). The ellipse is designed for the maximum brilliance transfer from the cold source to samples with surface areas between 5×5 mm^2 and 10×10 mm^2. The focussing effect is demonstrated in Fig. 4 (left) showing the intensity distributions in the focal point at the sample position for different length of the end section of the elliptic guide (see Fig. 3, top view). Fig. 4 (right) compares the presented setup with the situation where the horizontal elliptic guide is replaced by a constant cross section guide with the same coating (at the position of the sample of 10×10 mm^2 size), demonstrating a clear factor of 4 increase of the beam intensity for elliptic focussing.

The performance of the neutron beam delivery system of HERITAGE is presented in Fig. 5. The left panel shows the intensity-wavelength distribution simulated for a low wavelength resolution of $\Delta\lambda/\lambda$=10% at the entrance of the collimation base. The spectrum of the beam formed by the collimation slits S1 and S2 (see Fig. 3), both of 12 mm height at 4 m distance, i.e. at a beam collimation of 3 mrad (Boxcar), is depicted in the middle panel. The intensity integrated over the full wavelength spectrum amounts 7.6·10^9 n/cm^2/s (i.e. 5.4·10^8 n/cm^2 for each single pulse of the ESS).

The results from the simulations above are illustrated by the following simple estimations: (i) compared with the ILL, the average flux at the ESS with the TDR moderator is about equal; the chopping of the beam will result in losses of the useful neutron intensity due to the blocking of the neutron beam between the neutron pulses by the choppers; (ii) the opening time is defined by the ratio of the pulse width to their period that is approximately equal to 1/25; (iii) such pulse structure is naturally produced by the ESS, so no losses related to the time structuring of the neutron beam will occur; (iv) the flux gain due to the "pancake" moderator in comparison to the TDR moderator is about 2.5. Therefore, assuming that other beam parameters are similar, the expected gain is about 60. The actual gain may be even higher since a more advanced neutron optics is used at a newly build reflectometer.

The brilliance transfer of the whole neutron delivery system is shown in the right panel of Fig. 5. It is calculated by the intensity ratio virtually measured by two identical brilliance monitors (using the VITESS simulation package) placed directly at the position of the moderator with a cross section of 3×10 cm^2 (height×width) and at the sample position, respectively. Both monitors use an identical parameter set with the vertical and horizontal position set to 1×1 cm^2 and

Table 1
Basic guide design parameters: in order to avoid the depolarisation of the neutron beam, all guides are coated with non-magnetic super mirrors after the polariser (Section 4).

Section	Length [m]	Radius [m]	channels	Entrance [mm]		Exit [mm]		Coating in m		
			vertical	Width	Height	Width	Height	Left/Right	Bottom	Top
1	10.0	+400	5	95.8	30	194.5	30	3.0	3.0	40
2	1.0	∞	5	194.5	30	198.5	30	3.0	3.0	3.0
3	2.0	∞	5	198.5	30	202.7	30	3.0	3.0	3.0
4	4.0	∞	5	202.7	30	202.5	30	3.0	3.0	3.0
5	6.0	−400	5	202.5	30	180.5	30	3.0	4.0	3.0
6	4.0	−400	5	180.5	30	145.5	30	3.0	4.0	3.0
7	0.5	∞	5	145.5	30	140.0	30	3.0	3.0	3.0
8	2.0	∞	1	140.0	30	108.3	30	4.0	–	
9	1.0	∞	1	108.3	30	86.28	30	5.0	–	
10	1.0	∞	1	86.28	30	54.0	30	5.0	–	

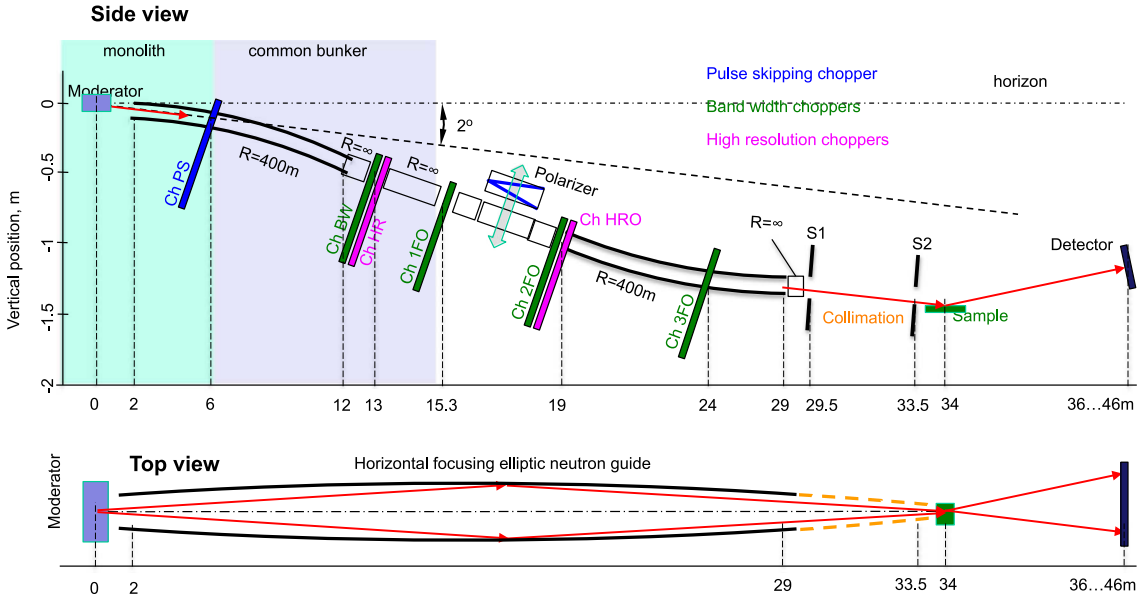

Fig. 3. The top and side view of HERITAGE. For clarity, the top view only shows the elliptic neutron guide. The end section of it (dashed brown lines) depicts a part of the collimation base and is exchangeable with other optical devices for different operational modes. The chopper design is given in [4]. (For interpretation of the references to color in this figure legend, the reader is referred to the web version of this article).

the vertical divergence to ± 0.9° (3 mrad), as used for the intensity calculation in Fig. 5. The horizontal divergence is restricted to the maximum divergence accepted by the ellipse on the entry side of ± 1.4°. The resulting brilliance transfer amounts to approximately 50% at λ=2 Å and saturates at around 75% for λ > 4 Å.

As stated above, the last 4 m of the horizontal elliptic neutron guide (Sections 8–10 in Table 1) is exchangeable: the elliptic end used for standard reflectometry measurements at solid substrates can be simply substituted by other modules e.g. by a liquid nose allowing to study free-liquid interfaces or a horizontal neutron collimation section to enable GISANS measurements. Such a modular design allows an extraordinary flexibility for the HERITAGE instrument with changes between the different instrument operation modes in minutes. The modular setup is described in more detail in the following sections.

4. Chopper modes: general, higher wavelength resolutions (1%, 3% and 5%) and pulse skipping

The chopper positions are depicted in Fig. 3. The first chopper BW at 13 m is the band selection chopper selecting an 8 Å broad wavelength band. The band from 2 to 10 Å will provide the highest intensity, however, the wavelength band can be selected arbitrarily in a range between 2 and 32 Å. The additional frame overlap (FO) choppers 1FO at 15 m, 2FO at 19 m and 3FO at 25 m prevent contaminations of neutrons with a wavelength of larger than 50 Å.

To allow for kinetic measurements (see Chapter 7) a pulse-skipping (PS) chopper is placed at a distance of 6.2 m downstream of the moderator directly after the biological shielding of the target. In combination with the PS-chopper the general chopper settings enable time resolutions of 140 ms, 210 ms and 280 ms by skipping 1, 2 or 3 pulses, respectively.

In order to achieve a high wavelength resolution for the proposed design, the natural pulse width has to be artificially reduced according to Eq. (1) and the wavelength frame multiplication (WFM) mode [8] is used to compensate for intensity losses. Technically the sub-pulse duration is defined by the pulse-shaping chopper HR installed at 13 m and the high-resolution overlap (HRO) chopper at 19 m distance from the source. The sub-frames that are well separated in time but overlap in their wavelength sub-bands are shown in Fig. 6. Consequently the available wavelength band from 2 to 10 Å is completely covered without gaps in Q.

Different resolutions require a variable opening of the pulse-

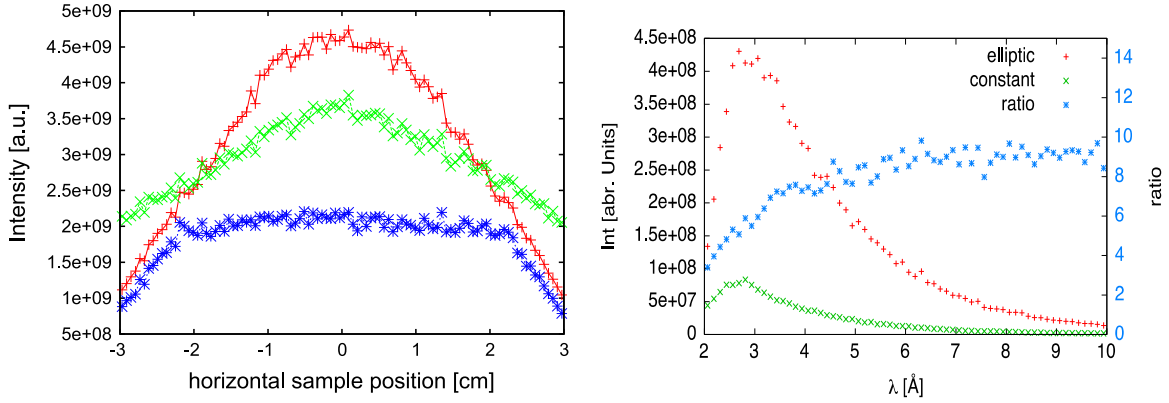

Fig. 4. Left: effect of focussing on the intensity distribution on the sample. Red curve (+) – full focussing by 4 m long end section of the elliptic guide, green curve (x) – focussing by 3 m long end section, blue curve (*) – focussing in the absence of the 4 m long end section, Red curve (+). Right: comparison of the intensity at the sample position with a sample size of 1×1 cm^2 for an elliptic and a neutron guide with a constant cross section. (For interpretation of the references to color in this figure legend, the reader is referred to the web version of this article).

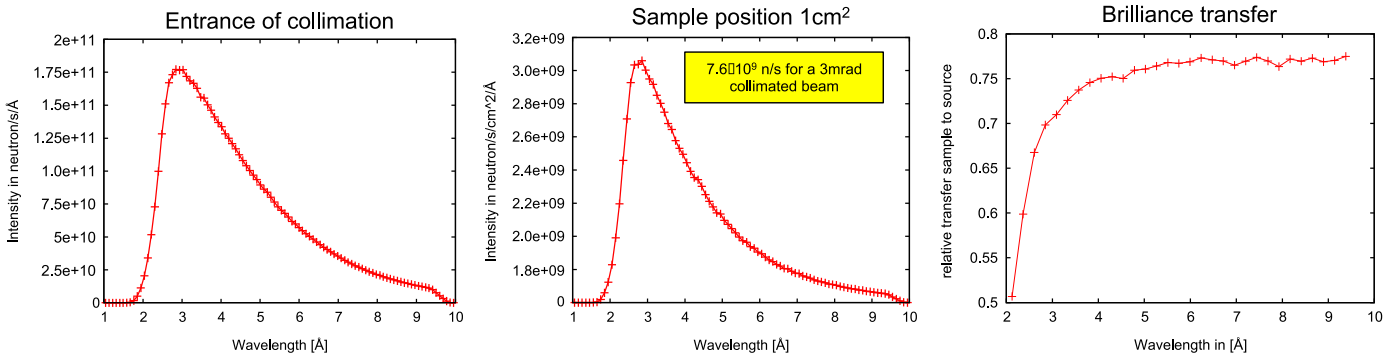

Fig. 5. Left: the intensity-wavelength distribution for the wavelength resolution of $\Delta\lambda/\lambda$=10% at the entrance of the collimation base (3×14 cm^2). Middle: the spectrum of the beam collimated to 3 mrad (Boxcar) in vertical direction on the sample. Right: wavelength dependence of the brilliance transfer of the whole neutron delivery system.

shaping (high resolution, HR) chopper. Therefore a double disc chopper allows for different openings by setting an offset angle between the discs. It is important to note that in all three modes (1%, 3% and 5%), the $\Delta\lambda/\lambda$ value is not constant since the pulse length, whether directly from the ESS or from the HM-chopper, is always constant, while λ changes.

A detailed description of the chopper design including the pulse skipping mode is given in [4].

5. Multi-beam setup for fast kinetics and the investigation of free standing liquids

5.1. Illumination from above

Wide Q-range reflectivity studies on free standing liquids in the TOF mode require 2–3 different incident angles onto the sample since the liquid surface itself cannot be tilted with respect to the horizontal direction. The latter is naturally possible when studying samples with solid-solid, gas-solid and liquid-solid interfaces.

It is furthermore important if not even essential to avoid any movement of the sample during and in between the experiments. The unavoidable vibrations would result in disturbances in the reflectivity profile or at least long waiting times between successive measurements. The idea of using multiple beams impinging on the sample under different incident angles for motion-free measurements at different Q values was realized at the V6 reflectometer [5] using the beams reflected from different crystals of vertically focussing monochromator and later at the REFSANS reflectometer [6] by bending the beam with the guide and the reflecting mirror. Recently it was put forward as the basis for the design of the FREIA reflectometer proposed for the construction at the ESS [7].

For HERITAGE, an alternative approach is suggested: three beams with the required inclination are selected from a conventional neutron guide in the scattering plane by deflecting mirrors (labelled as “Liquid-Nose”) while an elliptic (horizontal) neutron guide is planned to focus the neutrons onto the sample position perpendicular to the scattering plane. This allows HERITAGE to benefit from the enhanced flux due to the focussing features of the elliptic neutron guide and deliver significantly more neutrons onto the sample position as compared to using the approaches mentioned above. The horizontal focussing guide of HERITAGE provides a significant gain factor of about 5 with respect to a straight guide solution as e.g. in the FREIA concept [7].

The “Liquid-Nose” (see Fig. 7, left panel) setup is installed on a common support that can be moved in and out of the beam at the end piece of the collimation base replacing a 1.2 m long end section and part of the elliptic guide. Three beams illuminate the fixed horizontal sample under 0.3°, 1.1° and 3.7° and are used in a multiplex mode, i.e. one after another. As the position and the deflecting angle of the mirrors are adjustable, it is possible to select the most intense beam from the incoming divergence profile (see Fig. 8). The angular resolution and the footprint of the incident beam on the sample position are defined by the precision slits S1 and FS, respectively. The reflected intensity is detected by a position-sensitive detector (PSD) with an area of 1 m×1 m covering all three angles or a set of 3 independent single neutron counters to detect the specular and off-specular/background signal at the same time. Three fast shutters are installed in front of the deflecting mirrors which can be used for fast kinetic measurements on liquid interfaces. The cross-talk between single footprint slits in the FS is inhibited by 3 neutron absorbing apertures as it is shown in Fig. 7 (right panel). For normalization of

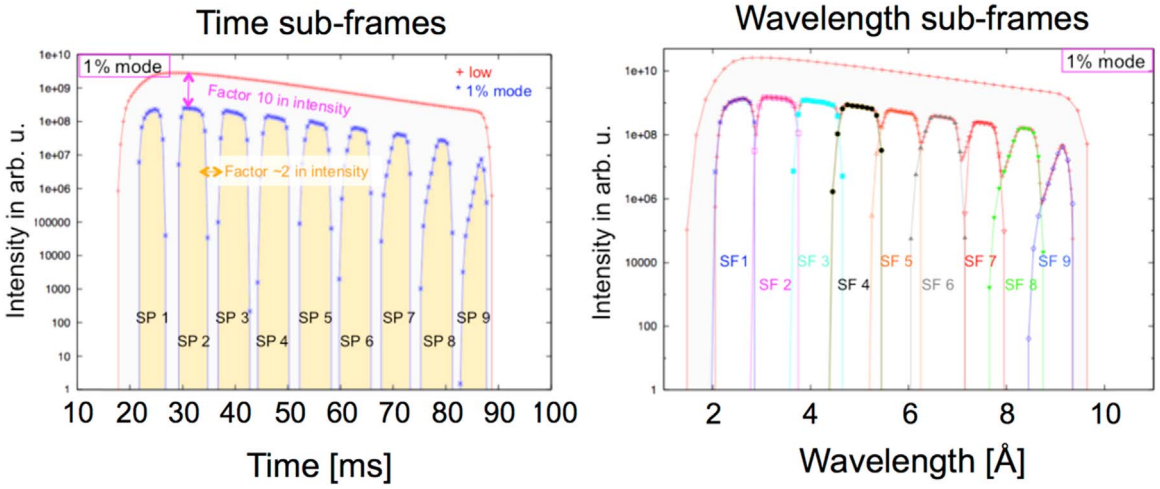

Fig. 6. The simulated time and wavelength intensity distributions for the 1% wavelength resolution modes. The low wavelength resolution curves ($\Delta\lambda/\lambda$=10%) are shown as envelops.

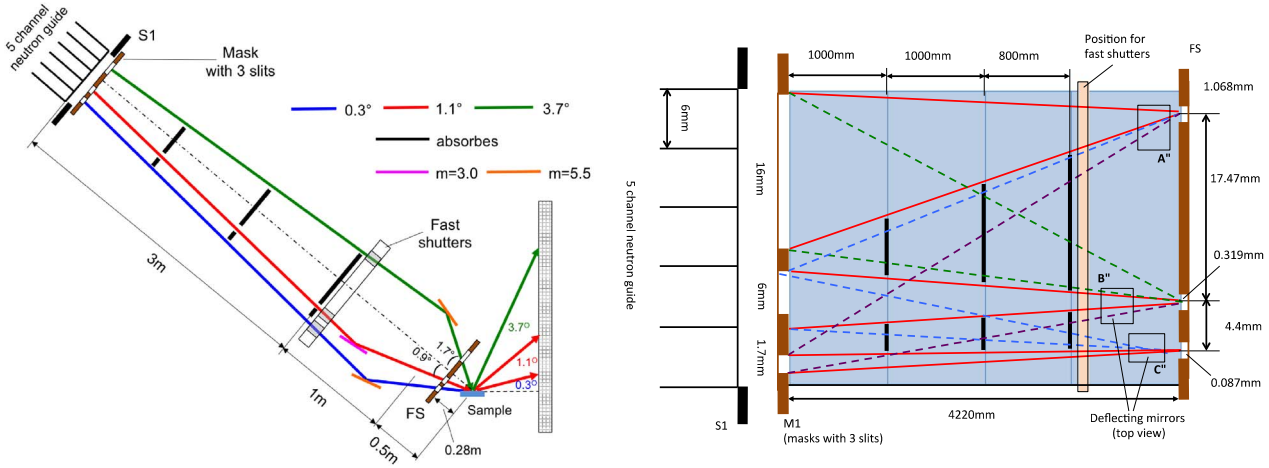

Fig. 7. Left panel: the sketch of the "Liquid-Nose". Blue, red and green lines depict the neutron beams impinging on the sample under incident angles of 0.3°, 1.1° and 3.7°, respectively. Black lines depict absorbers, pink and orange lines indicate the deflecting super mirrors with m=3 and m=5.5, respectively. Note, that the angles are intentionally increased for the sake of clearer visualisation. In reality all transmitted and reflected beams will be covered by the detector, placed in a distance shorter than 6 m from the sample. Left panel inset: the positional intensity distribution on the sample. Right panel: The top view of the "Liquid-Nose". Red lines depict the "useful" neutron beams, blue, green and violet lines are parasitic beams blocked by absorbers shown by black lines. (For interpretation of the references to color in this figure legend, the reader is referred to the web version of this article).

liquid reflectivity curve the direct beams intensities has to be measured. Therefore the sample has to be moved out and as a consequence the direct beams intensities are probed after the sample investigation, to prevent any movement of the sample. The PSD with an area of 1 m×1 m placed at a distance of 6 m from the sample covers a solid angle large enough to detect all transmitted and reflected beams without any vertical movement.

The Q-ranges corresponding to the angles 0.3°, 1.1° and 3.7° with a minimum and maximum wavelength of 2 Å and 9.5 Å, respectively, overlap well and enable access to a Q-range from 0.007 $Å^{-1}$ to 0.405 $Å^{-1}$ without moving the sample (Fig. 9 (left panel)). As an example, the neutron flux delivered onto a 40×40 mm^2 sample area at an incidence angle of 3.7° is calculated for the under-illumination conditions (right panel) and for an angular and wavelength resolutions of 4% and 10%, respectively. For the purpose of comparison, the slits and beam parameters are chosen as used in the ESS FREIA proposal [7] for an identical sample. The comparison clearly demonstrates a gain factor of about 5 as expected due to the focussing effect of the horizontally focussing elliptic guide (as discussed in Section 3) (see Fig. 4).

5.2. *Illumination from below (inverted sample geometry)*

In the "illumination-from-below" operation mode free-standing liquid or liquid-liquid interfaces can be accessed from below the interface. The HERITAGE design provides a unique possibility to carry out such experiments without moving the sample during the measurements. For this purpose the "illumination-from-below" setup (see Fig. 10) is moved into the beam.

The beam deviated by 0.2° is selected and collimated by the slits S1 and S2. This beam is deflected upwards by one of 3 super mirrors (labelled as **A-A′, B** and **C)** creating beams incident on the sample at the angles θ_{in}=0.33°, 0.8° and 1.8°, respectively. The reflectivity curve is measured subsequently in three steps, covering a total Q-range from 0.007 $Å^{-1}$ – 0.197 $Å^{-1}$ (Fig. 11) without vertical movement of the sample during the experiment. The Q-range can be even extended to 0.4 $Å^{-1}$using the mirror A installed 300 mm upstream the sample position that deflects the incident beam with an incident angle on the sample of θ_{in}=3.6°: As long as m=9 mirrors are not available, it can be replaced by an m=7 mirror allowing for a maximum Q value of 0.3 $Å^{-1}$..

Using the "illumination-from-below" setup in the under-illumination-configuration (for details see Section 10) given in Table 2 for a 40×40 mm^2 size large sample with an angular resolution of 4% will result in an intensity distribution on the samples as depicted in Fig. 10 (right). It demonstrates that the intensity distribution along Q for the individual angular settings possess a well-defined overlap. The slightly lower performance compared to the one for the "Liquid-Nose" setup is accounted for the reduced focussing effect since the elliptic guide ends already in front of the collimation (see Fig. 4) and two mirrors are required for the **A**-configuration instead of one in the "Liquid-Nose" case. The right panel of Fig. 10 clearly shows that for all three configurations the neutrons hit the sample at the same position and

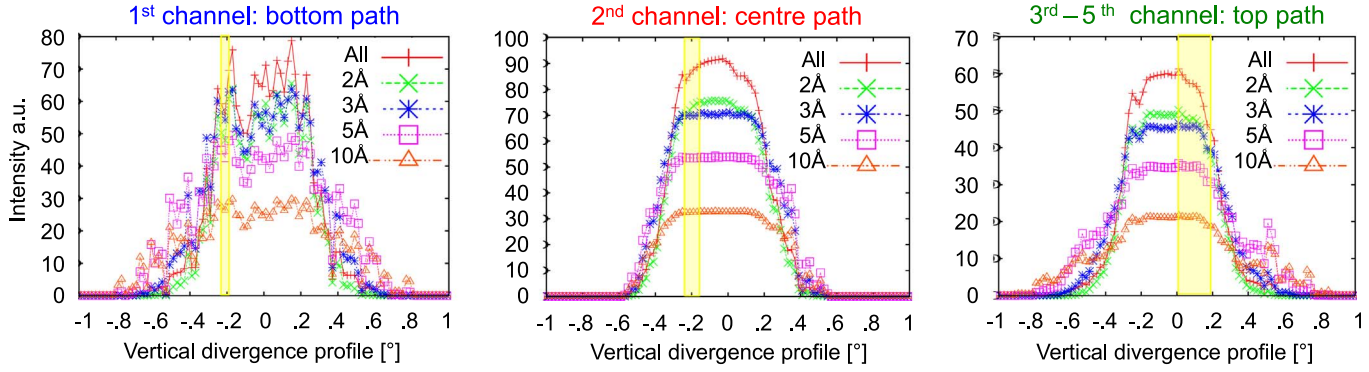

Fig. 8. Divergence profiles of 3 beams at the entrance of the "Liquid-Nose". Colour code corresponds to different wavelengths in the spectrum. Yellow bars are indicating the angular width of vertically collimated beam selected by mask M1 and slits FS. (For interpretation of the references to color in this figure legend, the reader is referred to the web version of this article).

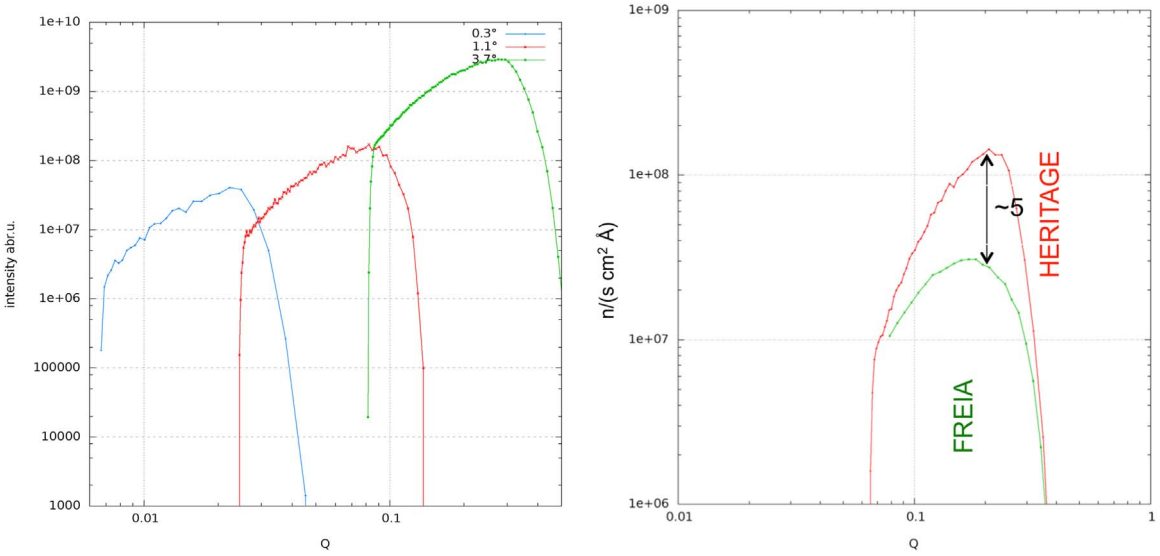

Fig. 9. Left: The Q-ranges covered by the incident angles 0.3°, 1.1° and 3.7°; the total accessible Q-range spans from 0.007 Å^{-1} to 0.405 Å^{-1}. Right: the comparison of simulated intensity delivered by HERITAGE and FREIA at an under-illuminated sample of 40×40 mm^2 for 4% angular and 10% wavelength resolutions for the incidence angle of 3.7°. The data for FREIA are taken from [7].

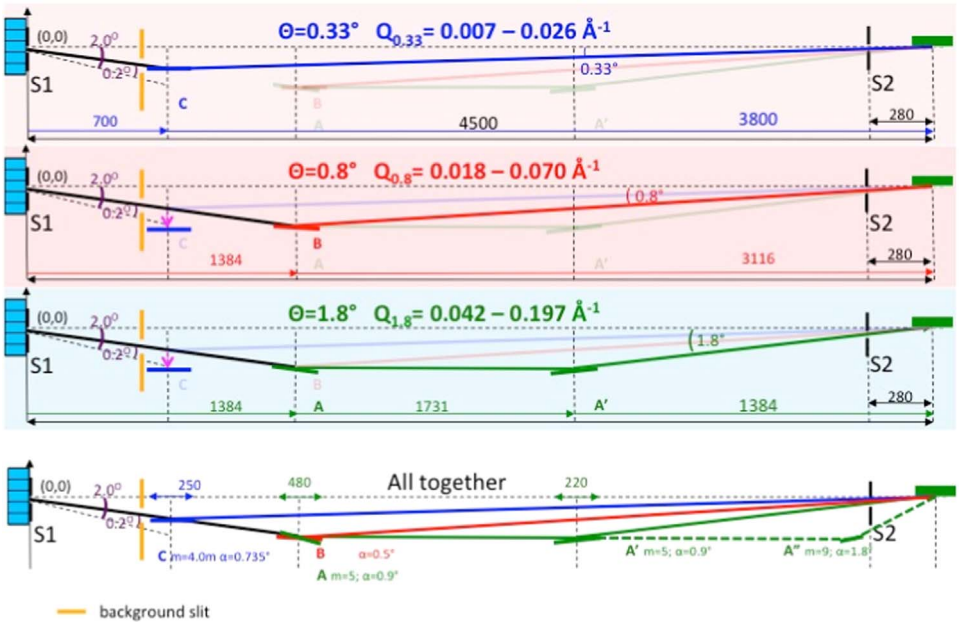

Fig. 10. Sketch for illuminating the sample from below. In the case of the 0.8° and 1.8° setup the mirror **C** is moved out of the beam. Furthermore mirrors **B** and **A** are identical so that only the inclination to the beam is changed. When using the configuration **B** or **A-A′** mirror **C** is moved out.

no additional (vertical) movement of the sample is required.

6. GISANS mode: the key element to the exploration of 3d-structures in thin films

The GISANS geometry requires a tight pinhole collimation not only in the vertical but also in the horizontal direction. This results in a significant loss of incident intensity of about a factor 30 with respect to the reflectivity mode. The intensity, however, can be strongly increased by using a number of sub-beams focussing onto the same point in the detector plane (see Fig. 12) [6]. In this case the resolution of the GISANS setup will not be defined by the collimation of the incident beam as in conventional SANS, but as the ratio of the beam spot size d_s in the detector plane to the sample-detector distance L_{SD}. The maximum Q-range of the GISANS setup is determined by the maximum detectable diffraction angle.

The size of the focal spot d_s (4 mm, 8 mm or 16 mm) for different sample-detector distances given in Table 3 is defined by the vertical slit sizes of masks M_1 and M_2 chosen for obtaining the required spot sizes d_s in the detector plane (see Section 10). A crosstalk between sub-beams is prevented by a set of one radial collimator and six comb-like masks providing a convergent neutron beam. They are placed inside the collimation base replacing the complete 4 m end section of the elliptic guide (Fig. 12). Mechanically, the positions of collimator and masks are fixed inside the modular unit and allow the GISANS option to be quickly moved out of the beam.

A detector of size 100×100 cm^2 and with a resolution better than 4 mm^2 is planned to be installed inside a vacuum detector tube. It is movable from 2 m to 12 m distance range with respect to the sample position. Note, that the detector resolution in the horizontal direction should match the above calculated d_s for the highest resolution or should be better by a multiple of integers. The polarisation analyser

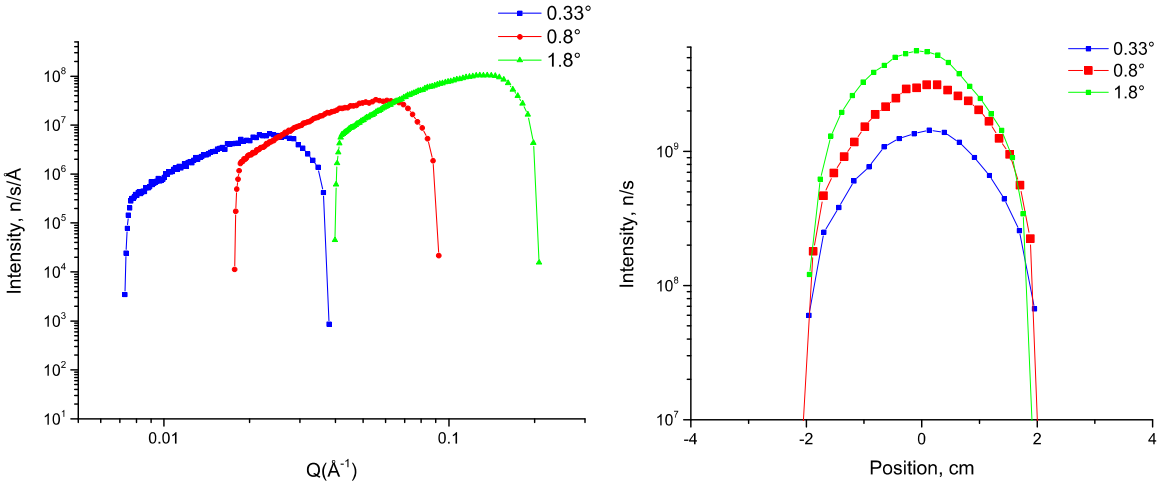

Fig. 11. Left panel: the Q-range overlap of the **A-**, **B-** and **C-**configurations. Right panel: the positional intensity distribution on the sample. Both simulations performed in the under-illumination configuration (Q_{theta}=4% resolution) for the slits settings shown in Table 2.

Table 2
Opening of the slits S1 and S2 in the vertical and horizontal direction for a 40×40 mm^2 sample (Q_{theta}=4% resolution) in the under illumination condition. The distance between S2 and the sample is 280 mm and between S1 and S2 it is 4220 mm..

θ, deg	S1 vertical	S1 horizontal	S2 vertical	S2 horizontal	S2-sample
0.33	1.944 mm	136 mm	0.096 mm	28.11 mm	280 mm
0.8	4.714 mm	136 mm	0.232 mm	28.11 mm	280 mm
1.8	10.61 mm	136 mm	0.521 mm	28.11 mm	280 mm

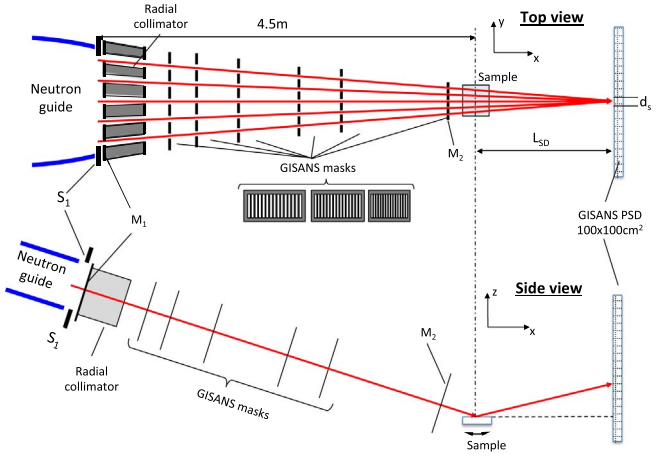

Fig. 12. Layout of the GISANS setup. Sub-beams propagating through comb-like masks M_1 and M_2 at distance of 4.2 m are focussed in the detector plane.

Table 3
Parameters of slits for selected GISANS settings.

S-D [m]	d_s [mm]	a_1 [mm]	b_1 [mm]	a_2 [mm]	Sub beams
2	16	14,81	19,42	5,19	4
4	16	7,89	7,27	3,97	9
8	16	4,08	3,02	2,70	19
12	16	2,75	2,69	2,05	25
12	8	1,37	2,69	1,02	34
12	4	0,69	2,69	0,51	41

(see Section 8) will be installed in the detector vacuum tube closer to the sample.

The intensity gain due to the multi-beam arrangement can be estimated as the ratio between the integrated area of a single beam passing the mask M_2 and that of the combined beam at the detector position. It provides a gain factor equal to the number of sub-beams focussed in the detector plane.

The performance of such a multi-beam setup in its highest resolution (d_s=4 mm, L_{SD}=12 m) is illustrated by the simulations shown in Fig. 14. Plots at the upper panels demonstrate the effect of focussing on the path to the detector. Each of the collimated sub-beams contributes equally to the spot at the detector position. Mask M_1 contains 41 slits with a width of 0.69 mm separated by 2.68 mm. Mask M_2 contains 41 slits of 0.51 mm width separated by 2 mm (Fig. 13). These slits provide an exact illumination of the d_s=4 mm spot in the detector plane. The absence of any satellite peaks in Fig. 14 (upper right plot) clearly demonstrates that the selected number of masks and their positioning avoid any significant cross-talk between the slits.

The highest resolution of $Q_{y,}^{min}$=2.2·10^{-4} Å^{-1} is achieved by using 9.5 Å wavelength neutrons for a 4 mm spot size on the detector and at a sample-detector distance of 12 m. The maximum Q_y value of $Q_{y,}^{max}$ =1.5 Å^{-1} is accessed for 2 Å wavelength neutrons and at a sample-detector distance of 2 m. It enables one to probe an extremely wide range of length scales covering lateral structures from 0.5 to 2.8 μm (see Table 4). By accessing such large structures in the micrometre range the GISANS option of HERITAGE provides a large overlap in the length scales accessible with off-specular scattering that can be very beneficial for the investigation of systems that inherit nanometre and micrometre objects (e.g. magnetic domain evolution in an external magnetic field).

The large horizontal size of the neutron beam at the guide exit of about 140 mm permits the application of a large number of sub-beams. As an example, for a beam spot of 4 mm at the detector and a 12 m sample-detector distances, about 40 sub-beams can be used for the GISANS measurements (see Fig. 14, right panel). Such a large number of sub-beams will also compensate for the intensity losses if e.g. a high angular resolution is required and result in an enormous intensity gain

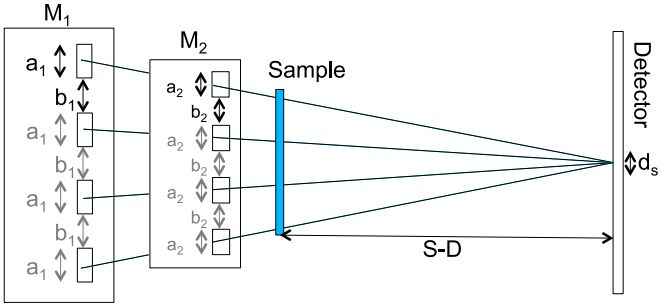

Fig. 13. Left: the geometry of the comb-like masks M_1 and M_2.

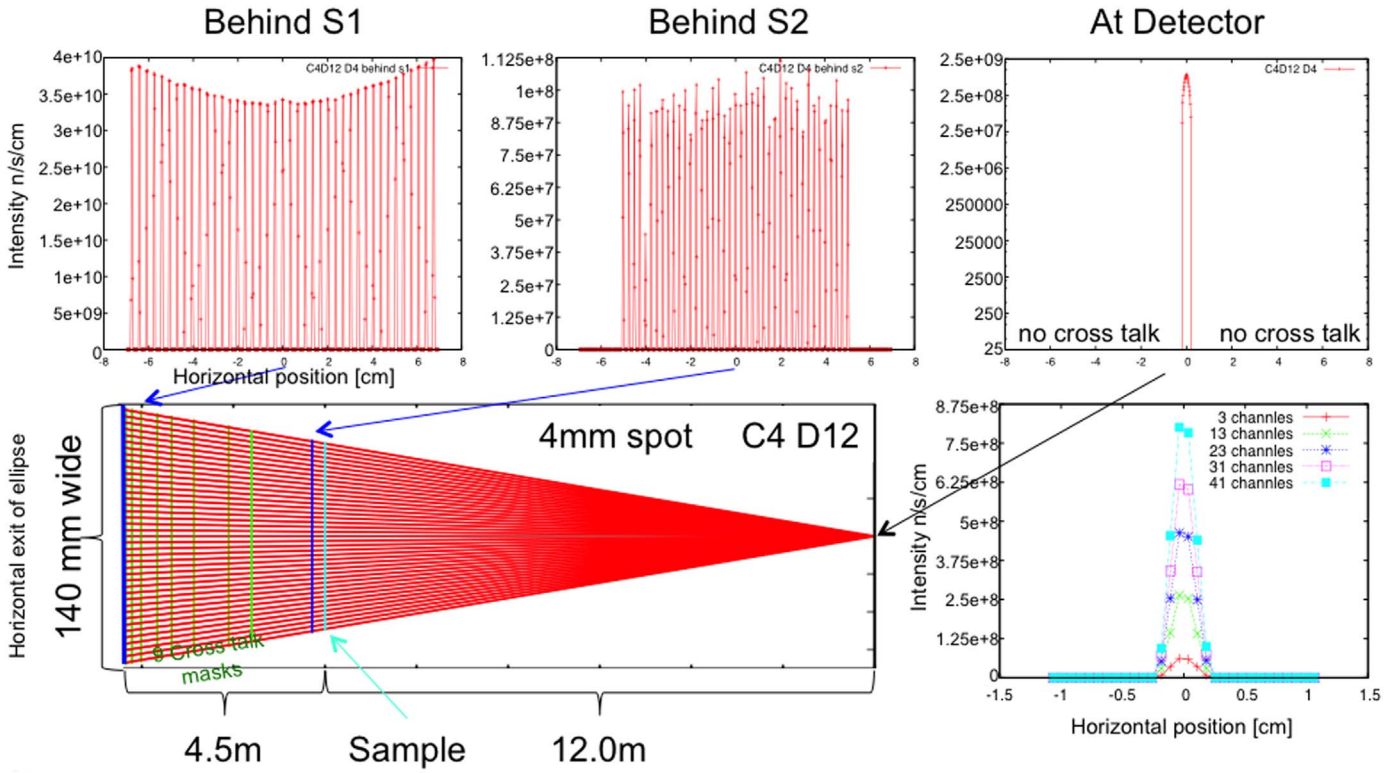

Fig. 14. Simulated performance of the GISANS setup for the highest resolution of HERITAGE (4 m long collimation length and 12 m long sample-detector distance). The gaps in the middle upper plot are due to poor simulation statistics in the narrow channels.

Table 4
Accessible lateral structures in the GISANS mode for minimum and maximum sample-detector distance for detector size of 100 cm×100 cm. The minimum Q_y is calculated from the Q-resolution, the maximum – for the detection at 100 cm from the incident beam axis.

Sample-detector distance	Size of the beam spot	Q_y^{min} (9.5 Å)–Q_y^{max} (2 Å)	Accessible lateral structures
2 m	16 mm	5.3×10^{-3} Å^{-1}–1.44 Å^{-1}	0.4 nm–120 nm
4 m	16 mm	2.6×10^{-3} Å^{-1}–0.77 Å^{-1}	0.8 nm–240 nm
8 m	16 mm	1.3×10^{-3} Å^{-1}–0.39 Å^{-1}	1.6 nm–480 nm
12 m	16 mm	8.8×10^{-4} Å^{-1}–0.26 Å^{-1}	2.4 nm–710 nm
12 m	8 mm	4.4×10^{-4} Å^{-1}–0.26 Å^{-1}	2.4 nm–1420 nm
12 m	4 mm	2.2×10^{-4} Å^{-1}–0.26 Å^{-1}	2.4 nm–2800 nm

relative to a pinhole arrangement with the same resolution. Comparing to a hypothetical TOF GISANS instrument at the ILL providing an angular resolution of 4 mm/12 m=0.33 mrad, the overall gain of intensity for HERITAGE can be rather conservatively estimated by multiplying the following factors: a factor of 25 due to the general intensity gain of the ESS in TOF mode, another 2 for the gain by the flat moderator vs. ILL cold moderator and a factor 40 due to the numbers of applicable sub-beams, thus resulting in an overall gain factor of 2000.

Increasing λ-resolution to 1% using the WFM mode [8] one can achieve high Q-resolution of about 1.5% by the cost of a factor of about 20 in respect to the low wavelength resolution mode [4] (see Section 3). Such a high Q_z-resolution allows for high-resolution depth profiling reflectivity measurements in thin films (see Fig. 2 in [10]).

The remaining intensity gain is still 100 as compared to existing SANS instruments which opens up an extremely exciting opportunity for GISANS studies. Trading intensity against a drastically increased $Q_{x,y}$-resolution allows to push the upper limit in GISANS studies to 2.8 μm (see Table 4) and to overlap the GISANS-covered length scale with the one by off-specular reflectivity measurements (1–30 μm). Combining the GISANS investigations with a high depth resolution opens the possibility for studies of 3d-structures in thin films in a single experiment - an area that is today inaccessible for neutron research due to the limited intensity.

It should be noted that in order to take full advantage of the multi-beam focussing GISANS mode, the sample has to be sufficiently large to intercept all possible sub-beams. In the case of the highest Q_y resolution (L_{SD}=12 m) the optimum sample size is about 100 mm, for a low Q_y resolution (L_{SD}=2 m) it is about 45 mm. The reduction of the sample sizes will result in a proportional reduction of the number of the usable sub-beams and thus of the intensity incident on the sample for the GISANS measurement.

One should further note that the increase of the sample-detector distance from 2 m to 12 m results in the narrowing of the Q_z-range covered in a single angular setting by 20% (2–7.5 Å), so that the angular shift between angular settings also has to be reduced by 20%.

7. Kinetic mode

HERITAGE is ideally suited for the performance of kinetic measurements on samples of 10×10 mm^2 or larger due to the high intensity delivered at the sample position. The kinetic mode is realized in two ways:

i) in the pulse skipping mode as described in the “Chopper modes” (Section 4).
ii) application of fast shutters as proposed by the FREIA [7] proposal of the ESS.

The first mode is best suited for solid based interfaces while the second option is particularly interesting for investigation of free standing liquid interfaces using the “Liquid-Nose” and its three beam geometry. The pulse-skipping mode is also suitable for latter and it may be used as a backup solution if the fast shutters fail.

The pulse-skipping mode as well as the fast shutter solution can be easily combined with other modes as e.g. the high wavelength resolu-

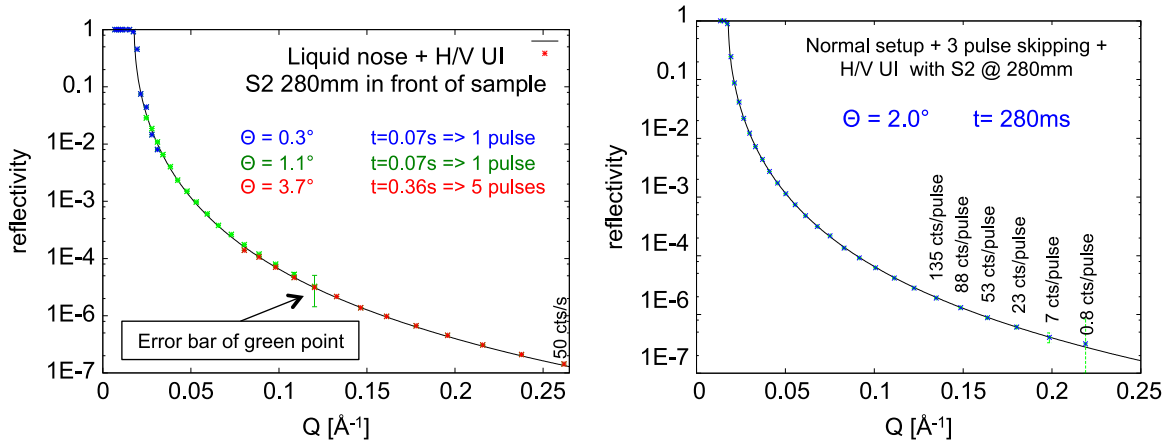

Fig. 15. Simulated reflectivity of a 40×40 mm^2 air-D_2O interface. Left panel: reflectivity curve at HERITAGE measured by "Liquid-Nose" at 3 incident angles using a fast shutter system in 7 ESS pulses (in 0.5 s). Right panel: the same curve measured by skipping three ESS pulses from a single ESS pulse at the incident angle of 2°.

tion mode or the GISANS mode and thus provides an extremely flexible experimental tool for studies of kinetics in nearly any sample environment. The optimization on high flux allows for ultra-short measurement times. The simulation of such a kinetic experiment on HERITAGE is shown in Fig. 15 for an air-D_2O interface with a surface area of 40×40mm2 measured with an angular resolution of 4%. The slit settings for the "under-illumination-condition" are given in Table 2.

In the fast shutter mode, a Q_z-range of up to 0.25 Å^{-1} is covered with all three angles in 11 pulses corresponding to a little more than one second total measurement time. At FIGARO [10], the highest flux reflectometer for the investigation of free-standing liquids at present, the measurement of a D_2O sample (with double size) for the same Q_z-range requires a total measurement time of 1 min, and a further minute is necessary for changing the guide configuration [7]. Thus, the gain factor for HERITAGE for such measurement is about two orders of magnitude. In the three pulse skipping mode a shorter Q_z-range up to about 0.18 Å^{-1} is covered with reasonable counting statistics, already in a time period of a single ESS pulse of 280 ms duration. Extending the Q_z-range to the range covered by the fast shutter mode, 20 s counting time is needed for reasonable statistics also up to high Q values. On the one hand, for free standing liquids this demonstrates the advantage of the fast shutter approach over the one by skipping pulses approach. On the other hand, for solid samples, the freely adjustable incident angle in the pulse skipping mode allows one to access nearly any Q value at which kinetics can be accessed. In such a way the two methods are complementary and enable one to flexibly study fast kinetics around low and high Q values in solids and in free standing liquids alike.

8. Polarisation and polarisation analysis

In the polarised beam mode, the central 1 m long piece of the 5-channel guide is replaced by a double channel polarising cavity (Fig. 16), which is built upon 0.3 mm thick, Si wafers coated with m=5 Fe/Si supermirrors operating in transmission. This solution leads to very high values of neutron beam polarisation (see Fig. 17) with small intensity losses over the entire wavelength band and it allows for the practically instant switch between the polarised and non-polarised beam operation modes without affecting the overall beam propagation. Even a higher polarisation of the neutron beam of above 99% can be achieved using an optional ^{3}He neutron spin filter, however, at the expense of a beam intensity loss of 25%. It should be noted that all sections downstream the polariser are coated by with non-magnetic super mirrors.

For the polarisation analysis a polarisation analyser can be placed between the sample table and the detector and can be quickly moved in and out. Different analyser types are foreseen for the different

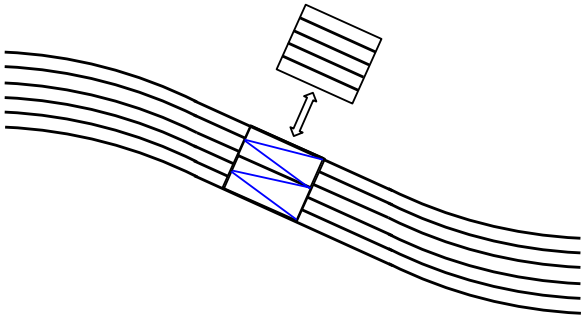

Fig. 16. Top view of the S-guide with the polarising cavity exchangeable with a non-polarising neutron guide section.

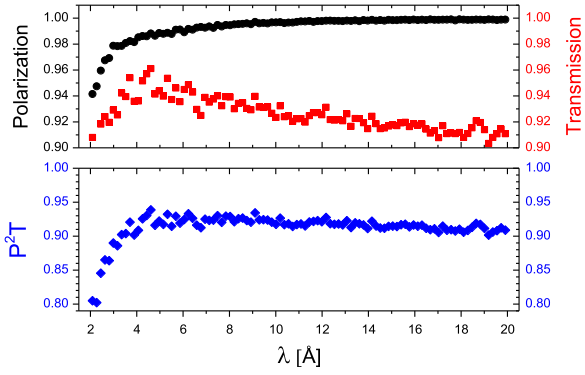

Fig. 17. Polarisation P, transmission T of the selected spin component and the figure of merit P^2T of the polarising cavity setup.

operation modes:

- For the specular reflectivity mode, when the detected beam has a rather small horizontal cross-section and angular divergence, a transmission analyser is used made of a double-side supermirror coated Si wafers. Upstream of the analyser an adiabatic RF-flipper is installed, providing extremely high flipping efficiency over the entire wavelength band.
- For the off-specular reflectivity and GISANS modes, when polarisation analysis should be performed over a wide solid angle range covering a large area of a position-sensitive detector, ^{3}He neutron spin filters are used as analysers Despite the variation of the transmission T of the ^{3}He neutron spin filters by a factor of about 5 over a broad wavelength band of 8 Å, the figure of merit P^2T changes only within 30% [11] so that the ^{3}He neutron spin filters can be used for TOF applications [12]. The application of on-beam

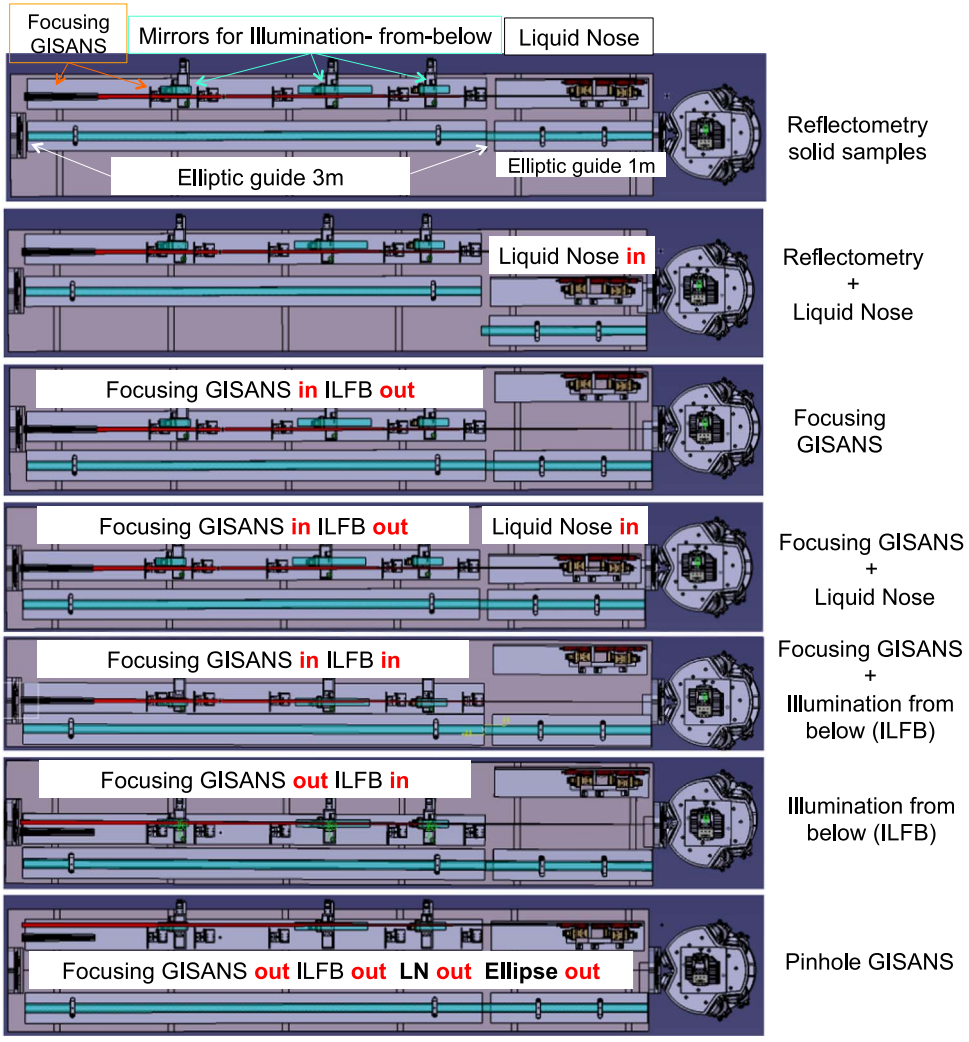

Fig. 18. A sketch illustrating the modularity of the different operational modes of HERITAGE. Optical elements – "Liquid-Nose", "GISANS", "Ellipse" and "Illumination from below" – move in and out sharing the space in the collimation base.

optically pumped large SEOP cells is here envisaged, where a very high degree of the polarisation (> 80%) is already achieved, resulting in a high transmission and polarisation efficiency over the entire wavelength band of about 8 Å [13,14]. Such a solution ensures the divergence of the scattered beam to be kept unchanged during the polarisation analysis. Moreover, the well-developed adiabatic fast passage technique allows for very effective flipping of ^{3}He spin states, thus no additional flipper after the sample is required.

It should be noted that while a polarisation analyser is essential for studies of magnetic samples, it is also extremely useful in reducing and in the end measuring the incoherent background created by hydrogen in soft matter samples.

9. Modularity

All the modes of HERITAGE described above can be freely and easily combined as depicted in Fig. 18. Additionally, the flexible wavelength resolution mode (10%, 5%, 3% and 1%), the polarisation and polarisation analysis, as well as the two (pulse skipping and fast shutters) kinetic modes can be combined with the reflectometry (specular and off-specular) mode as well as with the GISANS mode and even with the special liquid ("Liquid-Nose" and "illumination-from-below" modes) sample setup without any restriction. More than 20 different modes are thus feasible, each easily accessible and attainable in a few seconds.

10. Under-illumination of the sample

Avoiding any illumination of areas beyond the pure sample area in the sample plane, called the under-illumination of the sample, is extremely important for reflectometry and GISANS experiments since scattering from sample holders is a major source of background which is very hard to separate from the actual signal. The footprint slit FS controls the illumination of the sample by placing it at the distance L_s from the sample (Fig. 19).

Obviously the position L_s of the slit FS defines its size and therefore the intensity at the sample. The closer the slit FS is to the sample the less intensity is lost by the under-illumination condition. The minimum distance L_s to the sample is defined by the size of the sample environment around the sample. Hard matter samples are often to be studied at low temperatures and in strong magnetic fields, for which the typical sample environment is a closed cycle cryostats. A cryostat in which a 10 mm×10 mm sample can be easily placed has a typical outer radius of about 25 mm. For liquid samples, on the other hand, rather bulky environment are often necessary. For purposes of simulations in this article, L_s=25 mm for 10 mm×10 mm samples and L_s=280 mm for liquid samples with size 40 mm×40 mm are considered (Table 2).

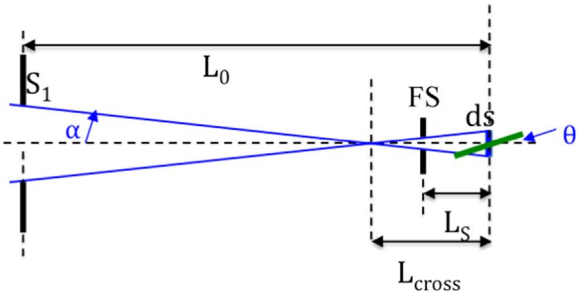

Fig. 19. Slit geometry (side view) for under-illumination of the sample (shown in green) with the effective size *ds*. For the horizontal direction the geometry is the same with *ds* equal to the actual width of the sample. (For interpretation of the references to color in this figure legend, the reader is referred to the web version of this article).

11. Measurements of extremely small reflectivities (up to 10^{-9})

The gain factor in neutron flux of about 60 provided by the HERITAGE design as compared to the today's strongest neutron sources in comparable conditions (e.g. using TOF at the ILL) offers great opportunities in the field of neutron reflectometry. It may lead to a drastic reduction of the measurement time, allowing for instance a detailed mapping of a phase diagram of a sample, which is not feasible today. In the field of kinetics, processes in the sub-second regime are accessible which is particularly interesting in a number of soft matter projects. The increase of neutron flux in combination with focussing techniques further allows investigating small samples down to 1 mm^2 sample surface or below.

Another big opportunity in neutron reflectometry inherent with such a drastic increase of the incident neutron flux is the ability to access lower reflectivities and a consequent extension of the accessible *Q*-range. Data from a larger reciprocal space regime will deliver direct and more accurate information about smaller lengths scales than it is possible today.

Assuming a background level *b* without time dependent (systematic) fluctuations and accounting for neutron scattering obeying Poisson statistics we consider only reflectivity signals above 3 times the fluctuation level of the background noise to be detectable. This leads to a relationship between the measurement time *t*, the lowest measurable reflectivity level *R* measured intensity from the specular part of the reflected intensity: $I_S = I_O R t$, the incident neutron flux I_O (neutrons per sec) and the background level *b* (background intensity: $I_{BG} = I_O b t$), as follows:

$$R = \sqrt{\frac{b}{I_0}\cdot\frac{9}{\mathrm{t}}} \qquad (2)$$

If we consider the ratio of the background level *b* to the incident neutron intensity I_O as a combined parameter and the time as another crucial parameter, the relationship between the lowest necessary counting time with respect to a signal of certain intensity (reflectivity level) can be illustrated as shown in Fig. 20.

By knowing the incident neutron flux and the background level *b*, the lowest reflectivity can be estimated. With a neutron flux of 10^8 n/s and a background level of 10^{-7}, for example, reflectivities of $R = 2\cdot10^{-9}$ are already measurable in 1 h or reflectivities of $R = 5\cdot10^{-10}$ in 12 h. The loss in incident neutrons can be proportionally compensated by a reduction in the background level if one wants to keep the measurement time constant. Having more incident neutrons, on the other hand, allows for a corresponding higher background as long as the ratio between *b* and *n* remains constant.

The considerations here imply that with the huge increase in neutron flux at the ESS and particularly with the HERITAGE concept, it is possible to measure reflectivities of the order of 10^{-9} or even below if the background level can be kept as low as here assumed.

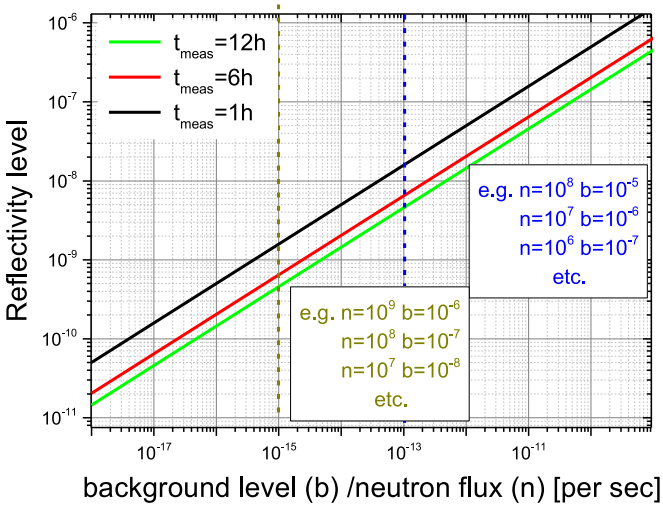

Fig. 20. The coloured full lines indicate the lowest measurable reflectivity level in respect to the relationship between the ratio of the background level *b* to the incident neutron intensity *n* for different measurement time *t*. (For interpretation of the references to color in this figure legend, the reader is referred to the web version of this article).

Theoretical intensity calculations for a sample system is illustrated in Fig. 21 to show how reflectivity levels of 10^{-9} can be measured in five hours or even less. It should be noted, however, that such low reflectivity levels require additional conditions to be fulfilled. At first, the incident neutron flux n on the sample is much lower at small than at large incident reflectivity angles due to the sample illumination condition. In case of samples with rough interfaces, the reflectivity drops already at very small incident angles to levels where the incident neutron flux is still too low for achieving a reasonable low b/n ratio that enables one to detect the signal. Second, and very crucial point: any systematic background components (which are impossible to measure independently) or statistical errors of time scales comparable to the typical measurement time are ignored and should be avoided. Such conditions make it impossible to distinguish the background from a weak signal. This latter condition, of course, is not limited to reflectometry, but is necessary to fulfil at any instruments at any neutron source. Therefore it is essential to place the experimental environment in an extremely stable environment, with respect to e.g. temperature or humidity changes that occur during the day/night cycle or other sources of long term external fluctuations. Moreover, it is essential to shield the experiment very well against parasitic neutrons stemming from neighbouring instruments, a possible major source of non-systematic, non-statistical background contribution.

12. Conclusions

The reflectometer concept presented here is not only supporting static and kinetic measurements on all possible types of interfaces (solid to free liquids) but combining unprecedentedly high flux with high lateral resolution allowing for the first time to investigate within one experimental session (several measurements) in a complete 3d-structural study of a thin film sample. The extremely high flux of $7.6\cdot10^9$ n/cm^2/s is achieved not only by the outstanding performance of the ESS pancake moderator but it is flanked by the modern neutron guide concept in the horizontal direction focussing on the sample via an elliptically shaped neutron guide. The intensity gain may be used just for achieving a significantly higher dynamic *Q*-range than feasible today, for considerably shorter time scale kinetic studies, for a higher *Q*-resolution, for the exploration of 3-d structure in thin films, for shorter measurement times or studies of very small samples at a reasonable time.

The strength of the HERITAGE concept lies in its potential to

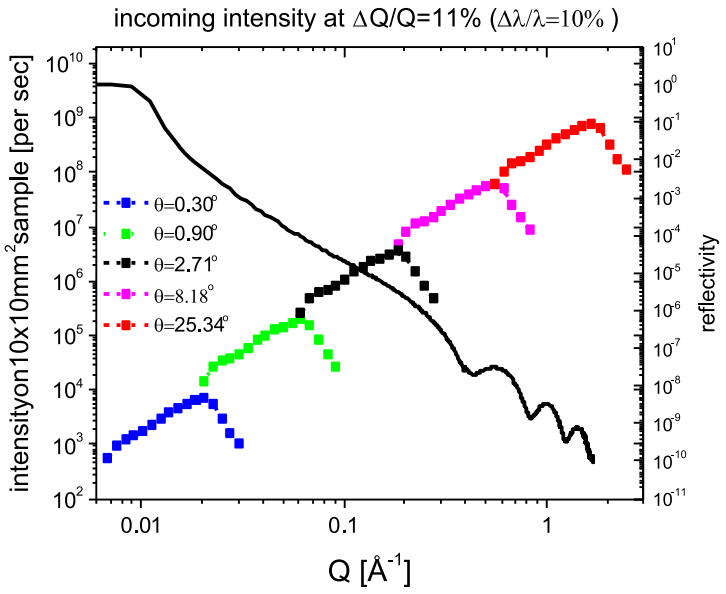

θ [deg]	Back-ground level	Reflecti-vity level	Time [sec, h]
0.3	$6{\cdot}10^{-7}$	$1{\cdot}10^{-2}$	1p
0.3	$1{\cdot}10^{-5}$	$1{\cdot}10^{-2}$	1s
0.9	$6{\cdot}10^{-7}$	$1.3{\cdot}10^{-4}$	1p
0.9	$1{\cdot}10^{-5}$	$1.3{\cdot}10^{-4}$	1s
2.71	$6{\cdot}10^{-7}$	$4{\cdot}10^{-6}$	1p
2.71	$1{\cdot}10^{-5}$	$4{\cdot}10^{-6}$	1s
8.18	$1{\cdot}10^{-7}$	$2{\cdot}10^{-8}$	1min
8.18	$1{\cdot}10^{-6}$	$2{\cdot}10^{-8}$	10min
25.34	10^{-7}	$1{\cdot}10^{-9}$	30min
25.34	10^{-6}	$1{\cdot}10^{-9}$	5h
25.34	10^{-7}	$1{\cdot}10^{-10}$	13h

Fig. 21. Left panel: incident flux for the various angular settings in consideration of the under-illumination condition for a wavelength resolution of 10%, aiming for a Q resolution of 11%. Right panel: theoretical calculation of the counting time for a 15 Å thick SiO_2 layer on Si substrate (without roughness) shown also in the left panel for different reflectivity levels vs. background levels of the real instrument.

investigate all kind of interfaces types by its ability to quickly switch between the available operational modes inside the collimation by keeping the complexity of the instrument low. HERITAGE operation range from single to multi-beam setups illuminating the sample from above or below allowing for the measurements of specular, off-specular reflectivity and GISANS modes combined with the full variety of λ-resolution, polarisation analysis and kinetic measurements.

The realisation of such a reflectometer concept provides an extremely high flux, far exceeding values at the currently best reflectometers in the world. The gain factor of about 2 orders of magnitude is expected in comparison with reflectometers at ILL and SNS [9,14,15,16]. Moreover, in comparison with the reflectometer design FREIA for ESS, the gain amounts to a factor of about 5 for 4×4 cm^2 liquid samples and to factor about 8 for gain for 1×1 cm^2 solid samples.

Acknowledgements

Authors would like to acknowledge the stimulating discussions with F.Mezei (ESS), R. Cubitt (ILL), Th. Brückel (FZJ), R. Dalgliesh (ISIS), K. Andersen (ESS), D. Argyriou (ESS), P. Müller-Buschbaum (TU Munich), J. Ankner (SNS), R. Pynn (UCSB) and L. Rosta (Wigner Research Center, Budapest).

We also would like to thank S. Manoshin (JINR, Dubna) for his support with VITESS.

References

[1] European Spallation Source Technical Design Report, 2013, ⟨http://eval.esss.lu.se/DocDB/0002/000274/014/TDR_online_ver_all.pdf⟩.
[2] K. Batkov, et al., Nucl. Instrum. Methods A729 (2013) 500–505.
[3] F. Mezei, et al., J. Neutron Res. 17 (2014) 101–105.
[4] S. Mattauch, A. Ioffe, D. Lott, A, Menelle, F. Ott, Z. Medic, J. Phys.: Conf. Ser. (2016) in press.
[5] F. Mezei, R. Golub, F. Klose, H. Toews, Phys. B: Condens. Matter 213–214 (1995) 898–900.
[6] R. Kampmann, et al., Physica B 385–386 (2006) 1161–1163.
[7] Instrument Construction Proposal FREIA, ⟨https://europeanspallationsource.se/sites/default/files/freia_proposal.pdf⟩.
[8] (a) F. Mezei, J. Neutron Res. 6 (1997) 3;
(b) F. Mezei, M. Russina, Advances in neutron scattering instrumentation, in: I.S. Anderson, B. Guerard (Eds.), , Proceedings of the SPIE 4785 (2002), 2002, p. 24.
[9] R.A. Campbell, H.P. Wacklin, I. Sutton, R. Cubitt, G. Fragneto, Eur. Phys. J. Plus 126 (2011) 107.
[10] P. Müller-Buschbaum, Polym. J. 45 (2013) 34.
[11] T.R. Gentile, et al., Physica B 356 (2005) 96–102.
[12] X. Tong, et al., Rev. Sci. Instrum. 83 (2012) 075101.
[13] W.C. Chen, T.R. Gentile, et al., J. Phys.: Conf. Ser. 294 (2011) NIST 3He.
[14] Z. Salhi, E. Babcock, P. Pistel, A. Ioffe, J. Phys.: Conf. Ser. 528 (2014) 012015.
[15] R. Cubitt, G. Fragneto, Appl. Phys. A74 (2002) S329–S331.
[16] Magnettism reflectomer at the SNS: ⟨https://neutrons.ornl.gov/mr⟩.